4.2

SENSITIVITY OF THE ATMOSPHERIC BOUNDARY LAYER AND CIRCULATION TO SEA SURFACE TEMPERATURES IN THE GULF OF CALIFORNIA: RESULTS OF MM5 MODELING STUDY

Dorothea C. Ivanova* and David L. Mitchell
Desert Research Institute, Reno, Nevada

1. IINTRODUCTION

The North American monsoon (NAM) is unique compared to other monsoon systems, because its northward expansion may depend on a warm current in spring moving up the Mexican coast, and its extension into the desert southwest of the United States may depend on sea surface temperatures (SSTs) in the northern Gulf of California (GOC) exceeding about 29◦C. Processes governing SSTs in the northern GOC may be complex. As a result of these processes, as well as other factors governing the general circulation in the monsoon region, certain monsoon seasons are more extreme than others in the desert southwest, and the onset of the summer rains exhibits year-to-year variability. Compelling evidence of the monsoon dependence on GOC SSTs is demonstrated through consistency between observational results and modeling study with realistic representation of the boundary layer (BL) and circulation. To test the dependence of the behavior of the monsoon BL on GOC SSTs, the model chosen should have a spatial resolution adequate for resolving GOC SSTs (e.g. the GOC is not resolved in most global climate models, or GCMs). In addition, the atmospheric model should treat monsoonal events as realistically as possible. Mesoscale models may be adequate for this purpose, and we have used the Pennsylvania State University / National Center for Atmospheric Research (PSU/NCAR) Mesoscale Model version 5 (MM5) as among the best for dealing with the complexity of this system. Moreover, the broad usage of MM5 in the atmospheric community allows other groups to repeat and expand upon our work.

We also note here that an earlier version of MM5, MM4, was used in Stensrud et. al. (1995) to simulate a monsoon season in a climatological sense. The simulation was consistent with observations, provided that the GOC SSTs were above 29◦C. The monsoon failed to fully materialize when GOC SSTs were lower than this. Since the climatological aspects of the NAM have already been successfully simulated by MM4, the focus of this study is to evaluate the sensitivity of the atmospheric boundary layer and circulation to SSTs in the GOC, using the results of the MM5 modeling work.

There are two main issues to be addressed in this paper. One concerns the debate about the GOC as a moisture source for the monsoon, exploring the idea that northern GOC SSTs exceeding about 29◦C could support favorable circulation and BL conditions at adjacent gulf regions and in the U.S. desert southwest. Our observational study supports the hypothesis that northern GOC SSTs play a critical role in the timing, amount and northern extent of the Mexican monsoon over the U.S. southwest (Mitchell et al., 2002). This hypothesis is now tested in a modeling context. The other issue is the prediction of the rapid increase in precipitable water over the N. GOC when SSTs increase from 29 to 30°C, apparently also related to the dilation of the marine boundary layer. MM5 allows us to simulate the general features of the Monsoon and to examine the changes in both: the tropospheric water content and circulation.

Model configurations, physical parameterizations used, and a description of the changes made to modify SSTs in different GOC regions are discussed in section 2. The experimental design, sensitivity experiments and simulation results are discussed in Section 3, while section 4 presents a summary and conclusions.

2. MODEL DESCRIPTION

As noted, the model used in this study is the PSU/NCAR MM5, the latest in a series that developed from a mesoscale model used by Anthes and Warner (1978). It includes multiple-nest capability, nonhydrostatic dynamics and a four-dimensional data assimilation capability (Grell and Dudhia 1994), which allow us to simulate the general features of the Monsoon. It is useful to first introduce the model framework, to define the coarse-grid and nest configurations and then to discuss the physical

*Corresponding author address: Dorothea Ivanova, Division of Atmospheric Sciences, Desert Research Institute, Reno, NV 89512; e-mail: dorothea@dri.edu

parameterizations that are used for the simulations.

a. Coarse-grid and nested-grid domains.
A two-way interactive nested procedure (Zhang et al. 1986), including most of the GOC, is shown in Fig. 1.

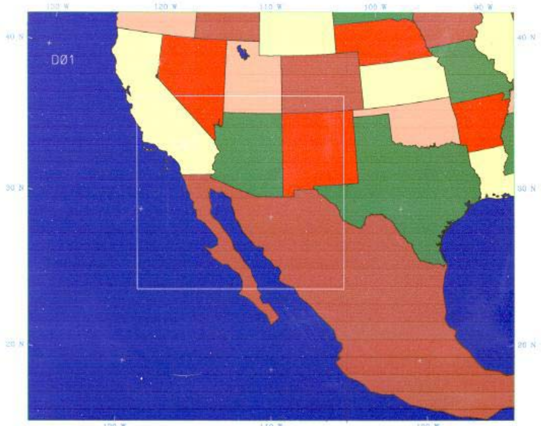

Fig.1 The nest and the coarse domain.

The nest domain obtains its lateral boundary conditions from the mother domain during the integration, and feeds the results back to the mother domain in the two-way nested application. The coarse-grid resolution is 90 km and the nested-grid domain has a horizontal grid spacing of 30 km. The vertical coordinate of the model is $\sigma=(p - p_t)(p_s - p_t)^{-1}$, where p is pressure, p_s is surface pressure, and p_t is the specified constant pressure at the top of the model (100 mb). The number of σ levels is 30, which gives 30 layers of unequal thickness at which the temperature, moisture, and wind variables are defined. The number of grid points in (x, y, σ) on the coarse-grid are: 45 x 51 x 30 and the number of grid points in (x, y, σ) on the nested-grid are: 49 x 52 x 30. The layers from the surface to near 700 mb are chosen to be approximately 20 mb thick to represent adequately the boundary layer. Above 750 mb the layers increase in pressure interval. A similar model configuration has been used by Stensrud et al. (1995) in their hydrostatic runs. The additional term in nonhydrostatic dynamics in MM5 is the vertical acceleration that contributes to the vertical pressure gradient so that hydrostatic balance is no longer exact. Pressure perturbations from a reference state together with vertical momentum become extra three-dimensional predicted variables that have to be initialized.
The two-way interactive nested grid procedure allows realistic representation of the complex terrain features of the Sierra Madre Occidental.

b. Physics parameterizations

The key problem of any mesoscale model is the calculation of the model physics.

• The Cumulus Parameterization (ICUPA) used in this study is the Grell scheme (Grell et al. 1994). It is based on the rate of destabilization or quasi-equilibrium; basically it is a simple single-cloud scheme with updraft and downdraft fluxes and compensating motion determining the heating/moistening profile. It is useful for smaller grid sizes and tends to allow a balance between resolved scale rainfall and convective rainfall, considering the shear effects on precipitation efficiency. As pointed out in a recent study (Gochis et al. 2001), different convective schemes (CPS) usage is appropriate across the North American Monsoon (NAM) modeled domain. Running a mesoscale model over the whole NAM region presents convective parameterization challenges, because different CPS's have assumptions and parameter specifications that make them more appropriate in some regions than others.
This is complicated over the NAM domain, which is of appreciable size. In our future work we will expand upon the sensitivity studies, using Kain-Fritsch scheme, which is the most physically complex and appears to generate convective precipitation more realistically in the north of the NAM region, according to Gochis.
As with the Kain-Fritsch scheme, in the Grell scheme used here, the convective mass flux is determined by the flux required to stabilize an unstable air column, but the closer assumptions differ in implementation between the two schemes.

• The Explicit Moisture Scheme (IMPHYS) is Simple Ice (Dudhia 1993). It adds ice phase processes to stable precipitation and warm rain schemes without adding memory — there is no supercooled water, and snow melts immediately below the freezing level. While this is run for efficiency and for summer cases, it performs better than Reisner mixed phase scheme for these conditions (Grell and Dudhia 1994).

• The Planetary Boundary Layer (PBL) Scheme (IBLTYP) is the MRF PBL scheme, also called the Hong-Pan PBL scheme. It is suitable for high resolution in the PBL (as for Blackadar scheme); an efficient scheme based on the Troen-Mahrt representation of the counter gradient term and K profile in the well-mixed PBL. Vertical diffusion uses an implicit scheme to allow longer time steps (Hong and Pan 1996). The sensitivity of the numerical simulations of the NAM BL to the choice of PBL turbulence parameterization in MM5 was tested in a study by Bright and Mullen (Bright and Mullen 2002). They found that the MRF (Hong-Pan) PBL and Blackadar PBL schemes correctly predict the development of the deep, monsoon PBL, and consequently do a better job of predicting the convective available potential energy and downdraft convective potential energy. The Burk-Thompson and Eta schemes do not accurately reproduce the basic structure of the monsoon PBL. To ensure accurate simulation of the monsoon PBL in conjunction with the accompanying model physics, we chose the MRF PBL parameterization.

• The Radiation Scheme (IFRAD) is a sophisticated cloud-radiation scheme to account for longwave and shortwave interactions with explicit cloud and clear air, as well as atmospheric temperature tendencies, which provides surface radiation fluxes (Hack et al. 1993).

The data used for initializing a simulation includes all available conventional surface-land, ship, buoy, and upper-air reports. The observational data are available every 6 hours for our case study with no missing data reports. The observational data are blended with first-guess fields of temperature, horizontal wind components, relative humidity, and sea level pressure global analyses from the NCEP (National Centers for Environmental Prediction) GDAS (Global Data Assimilation System), archived at NCAR (National Center for Atmospheric Research). Analyses are available every 12 hours. Data are archived on 2.5 degree x 2.5 degree latitude/ longitude grid in GRIB format. SSTs are archived once per day. The other available analyses (NCEP/NCAR Reanalysis, NCEP ETA, ECMWF TOGA Global Analysis and ECMWF Reanalysis) do not archive SST.
As pointed by Stensrud et al. (1995), the global SST data, used to initialize the PSU/NCAR mesoscale model, do not have sufficient horizontal and temporal resolution, and do not capture the dramatic warming of GOC SSTs during summer. Some modification in the treatment of GOC SSTs was a must in order to represent observed SST values and patterns in the GOC. New code was implemented in MM5 whereby SSTs in the four regions defined in our empirical study (Fig. 2) could be varied independently: northern gulf (N. Gulf), central gulf (C. gulf), southern gulf (S. Gulf), and another “pre-gulf region” immediately south of the mouth of the gulf.

Fig. 2 Four GOC and adjacent regions.

Our coarse grid includes all four GOC regions and all four adjacent regions as shown in Fig. 2.The nest comprises the Northern and the Central Gulf (regions C and D) and the regions adjacent to them.

During the twelve 72-h simulations, a four-dimensional data assimilation (FDDA) procedure was used to insert atmospheric data into the model through a Newtonian relaxation nudging procedure (Kuo and Guo 1989, Stauffer and Scaman 1990). Newtonian relaxation terms are added to the prognostic equations for wind, temperature and water vapor. By using data assimilation on the coarse mesh and nesting with a finer mesh, the fine mesh is provided with superior boundary conditions compared to the standard linear interpolation of analyses, because the boundaries have a much higher time resolution of features passing through them into the nest mesh. The assimilated fields were used as first-guess field for 0000 UTC, using all the available surface and upper-air data. These assimilated fields are superior to the operational global analysis on the base of more realistic upper-tropospheric jet structure (Kuo et al. 1995). To produce a realistic stable planetary boundary layer (PBL) and to allow the model fields to adjust to the underlying terrain surface, no temperature nudging is done in the PBL and all nudging coefficients are incrementally reduced to zero at 12 h of the nudging interval.   The assimilation period is complete at 1200 UTC and the model error introduced by the use of FDDA is restrained. The model simulations continue for another 60 hours and only the periods of actual model simulation are discussed in the following sections as simulation results.

3. EXPERIMENTS DESIGN AND SIMULATION RESULTS

a. Experimental design

As noted, we seek to examine the dependence of monsoon BL and circulation to variations in N. GOC SSTs. To examine this dependence in a climatological sense, we refer to the evolution of GOC SSTs described in Fig. 25 of our empirical study (Mitchell et al. 2002) and GOC SST values are tabulated for the various MM5 simulations in Table 1.

Table 1. MM5 model experiments: SST values correspond to the evolution of GOC SSTs based on June-August climatology.

Simulation number	SST in the Northern GOC	GOC SST south of the archipelago
1.	22°C	24°C
2.	24°C	26°C
3.	25°C	27°C
4.	26°C	28°C
5.	27°C	29°C
6.	28°C	30°C
7.	29°C	30°C
8.	29.5°C	30°C
9.	30°C	30°C
10.	31°C	30°C
11.	31.5°C	30°C
12.	32°C	30°C

Simulations 1-6 maintain a SST difference of 2 ^{o}C between the N. GOC and GOC regions south of the island region, or archipelago, as regions south of the archipelago warm from 24 ^{o}C to 30 ^{o}C. This is similar to the observations in Fig. 25 of the empirical study, except the differential of 2 ^{o}C is somewhat less in the empirical study when 30 ^{o}C is reached south of the archipelago. But since such conditions can occur, we wanted to account for such differences and to provide a strong test regarding the role of N. GOC SSTs on AZ boundary layer. That is, the likelihood of GOC regions south of the archipelago affecting AZ BL should increase, as their SSTs increase, and the effect of N. GOC SSTs would have to be strong to impact mixing ratios associated with 30 ^{o}C water under southerly flow. Once GOC regions south of the archipelago attain 30 ^{o}C, the SST difference between the N. GOC and regions to the south erodes until N. GOC SSTs exceed SSTs to the south. During the 1996 and 1997 monsoon seasons described in the empirical study, N. GOC SSTs almost reached 32 ^{o}C for a week. But the main reason for simulations 11 and 12 is to explore the behavior of deep circulation and increasing the depth of AZ BL over the broadest range of N. GOC SSTs.

Now that the strategy for examining the evolution of GOC SSTs has been described, we will introduce the atmospheric conditions assumed. The purpose of this study is not to examine all atmospheric conditions during a typical monsoon season, but to examine a single gulf surge event which is representative of low-level flow conditions leading up to and during periods of AZ rainfall (Stensrud et al. 1997; Fuller and Stensrud 2000). For this purpose, we have selected the gulf surge event studied in Berg et al. (2000), which resulted in the Las Vegas flash flood of 8 July 1999. While the Vegas flood was unusual, the widespread rainfall over AZ on July 7th was more typical of monsoon conditions. Therefore MM5 was initialized for conditions at 00 UTC on July 5th, with simulations run for 72 hours, up to 00 UTC on July 8th, just prior to the Vegas flood. By simulating conditions during a gulf surge event, we hope to examine the dependence of AZ BL and circulation during favorable atmospheric flow conditions as a function of climatological GOC SSTs. By restricting atmospheric conditions to those conducive for this specific AZ event, we can isolate the impact of GOC SSTs on AZ BL, mixing ratio and circulation. Hence, all MM5 simulations are identical except for the GOC SSTs assumed.

The target region over which rainfall amounts were assessed is a cross-section, perpendicular to the mid-N. GOC. It extends from 118° W (in Pacific Ocean) – all the way through the N. GOC and through southern Arizona to New Mexico at 109°W. This region is similar to the Arizona-New Mexico region described in our empirical study, but is not identical. It captures much of the region of rainfall resulting from the gulf surge events, and focuses on AZ since we are primarily concerned with the impact of N. GOC SSTs on the evolution of AZ PBL . PBL evolution, circulation, mixing ratio and potential temperature cross-sections for a 72-hour simulation were determined for this region.

To follow the described parallel with the empirical study, we selected for our numerical experiments as a case study the heavy monsoonal rains in Arizona, prior to Las Vegas flash flood of 8 July 1999. The flood event of 8 July occurred 2 days after the 29◦C threshold of the SSTs was exceeded, thus allowing us to study the role of the SSTs in the timing and evolution of the monsoon event. Although normally fixed (from observations), a 'do loop' for incrementing SSTs is implemented into one of the MM5 decks, such that SSTs in the different regions of the GOC could be modified. Twelve 3-day simulations were made with each simulation increasing the SSTs in the Northern Gulf of California with 0.5◦C to 1.0◦C, keeping at the same time SSTs in the other GOC regions at a fixed value. MM5 simulations were performed for the period July 5 - 8, 1999, beginning and ending at 00 UTC. In real life, no rain occurred on the 5th (MST), but rain occurred in AZ in early evening on the 6th and throughout the remainder of this period, which is examined for favorable BL and circulation conditions.

b. Results and discussion

All simulations 1 to 6, as described in Table 1 produced very similar output fields for BL, circulation, mixing ratio and potential temperature before 48 Z. After that period the changes that occur are also very consistent for these simulations. We will examine here simulation 4 (SSTs in the N. GOC 26°C and GOC SSTs south of the archipelago at 28°C) as representative for this group of simulations. A change in the deepening of the BL and circulation is observed at 36Z and 48Z for simulation 7 (SSTs in the N. GOC 29°C and GOC SSTs south of the archipelago at 30° C), but the most dramatic changes in circulation, mixing ration, BL depth and potential temperature occur at 36Z, 48Z and 72Z for simulation 9 (SSTs in the N. GOC 30° and GOC SSTs south of the archipelago also at 30°C). Simulations 10, 11 and 12 produced output fields for 35Z, 48Z and 72Z similar to simulation 9.

The examined cross-sections show very similar wind fields before 36Z (5 am MST). At 36 Z the updrafts for simulation 7 (Fig. 4) extend higher at 580 mb above the N. GOC compared to the updrafts for simulation 4 (Fig. 3), where the updraft approaches 620 mb only.

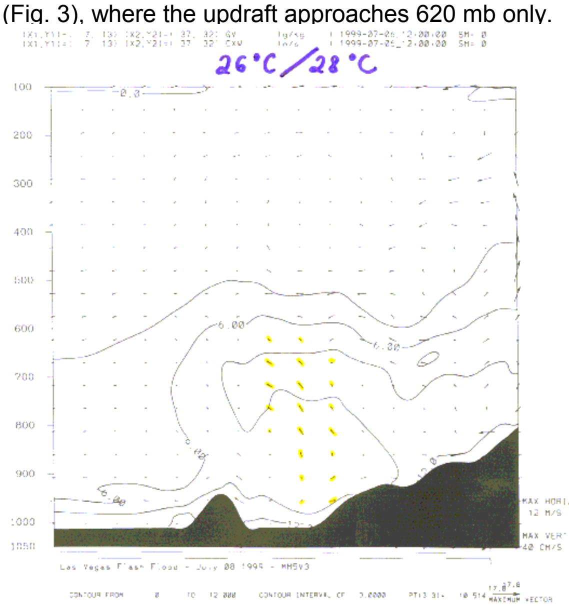

Fig. 3 Simulation 4: 36Z,SW-NE cross-section of mixing ratio (g/kg) and circulation updraft vector (m/s)

The mixing ratio (Qv) values from the same output fields are also very similar before 36Z, but at 36Z mixing ratio values over N. GOC become higher for simulation 7.

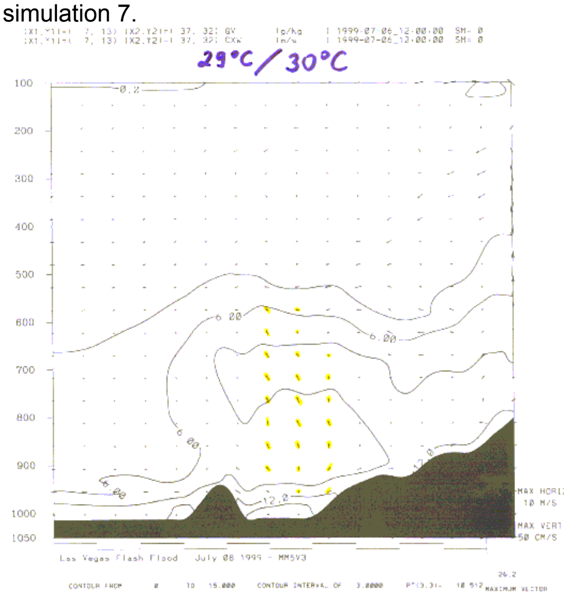

Fig. 4 Simulation 7: 36Z, SW-NE cross-section of mixing ratio (g/kg) and circulation updraft vector (m/s)

Mixing ratio over the GOC becomes much higher for simulation 9 (SSTs in the N. GOC 30° and GOC SSTs south of the archipelago also at 30°C) for 36 Z, but main differences between the previous simulations and simulation 9 occur at 48 Z and 72 Z.
This apparently is not due to drainage winds, leaving SSTs (warm relative to land) as the likely culprit. These higher winds deepen the moist BL over N. GOC.
Note, that winds at 42Z are onshore at low levels. This pumps GOC moisture inland at 42Z, and although wind fields at 42 Z are still very similar, the dramatic change is observed at 48Z (Fig.5 and Fig.6)

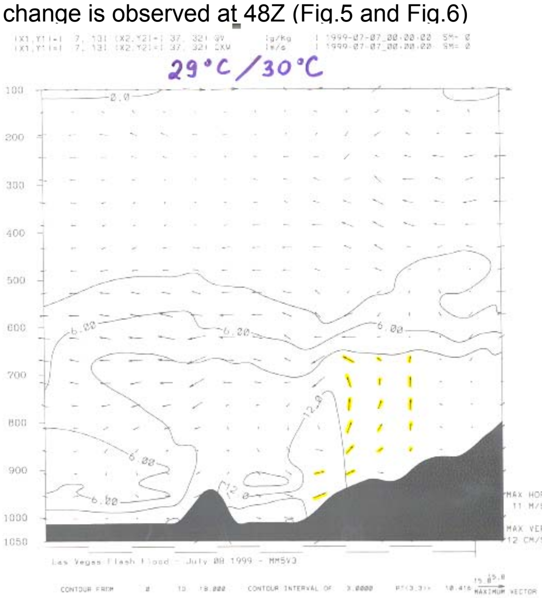

Fig. 5 Simulation 7: 48Z, SW-NE cross-section of mixing ratio (g/kg) and updraft vector (m/s)

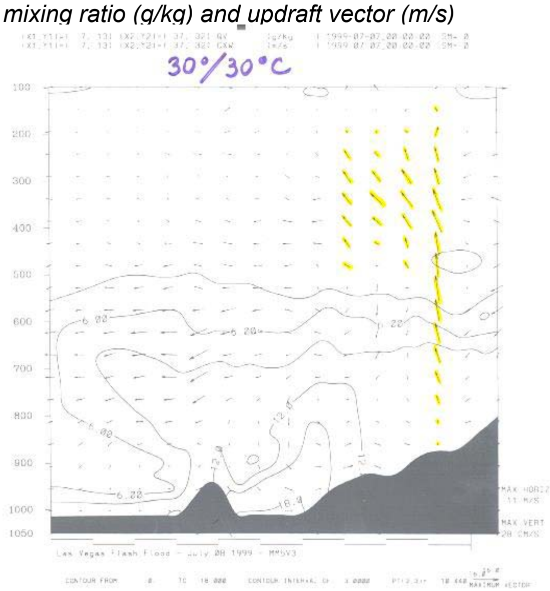

Fig. 6 Simulation 9: 48Z, SW-NE cross-section of mixing ratio (g/kg) and updraft vector (m/s)

The output fields for 48Z are indeed much different. Low-level convergence zone over the mountains is more inland with updrafts twice as big for simulation 9 (Fig. 6). Mixing ratio values continue to be higher over the N.GOC for simulation 9, with contours modified by the winds. These differences occur only over GOC and surrounding terrain at lower levels. Rainfall is stronger and close to the ground for simulation 9, while rainfall evaporates far above the ground from smaller cells in simulation 7. Actually the first significant rainfall occurs at 48Z for simulation 9. Cloud water fields are very similar before 48Z and slightly more extensive for simulation 9 at 48Z. Higher mixing ratios penetrate deeper inland for the 30°C N. GOC simulation (Simulation 9). They are apparently responsible for the main rain cell over lower terrain near GOC.

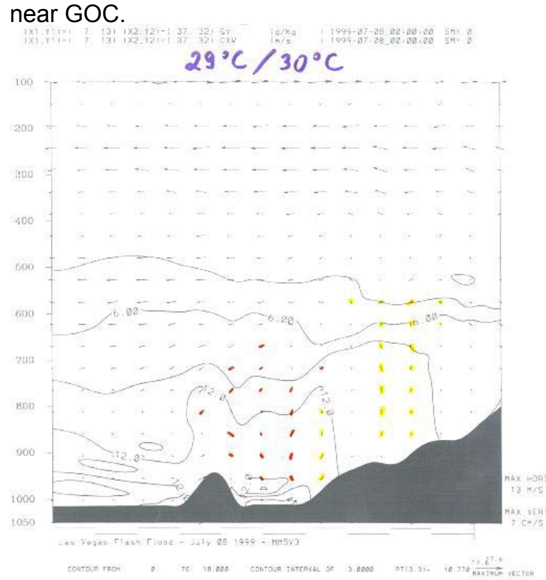

Fig.7 Simulation 7: 72Z, SW-NE cross-section of mixing ratio (g/kg) and updraft vector (m/s)

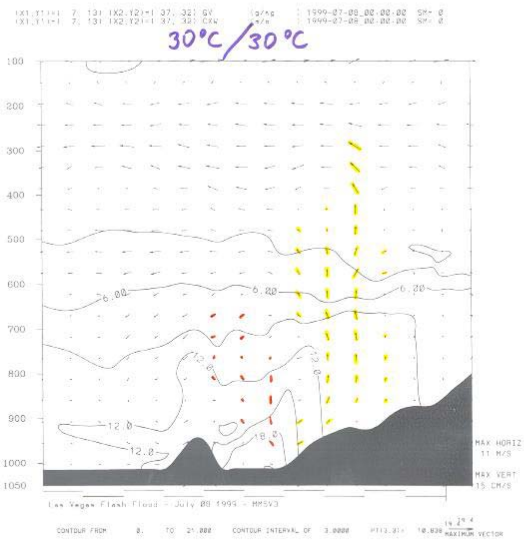

Fig. 8 Simulation 9: 72Z, SW-NE cross-section of mixing ratio (g/kg) and updraft vector (m/s)

The output fields for 54Z, 66Z and 72Z show as before – wind cycle over GOC and mainland much stronger for simulation 7 compare to simulation 4 and strongest for simulation 9 (Fig. 7 and Fig. 8)

Strong drainage winds are building and deepening the BL and the moisture over GOC, but the updraft is not further inland as before. Higher mixing ratio values are not as far inland either for 72Z, versus 48Z, but cloud water and rainwater fields are more

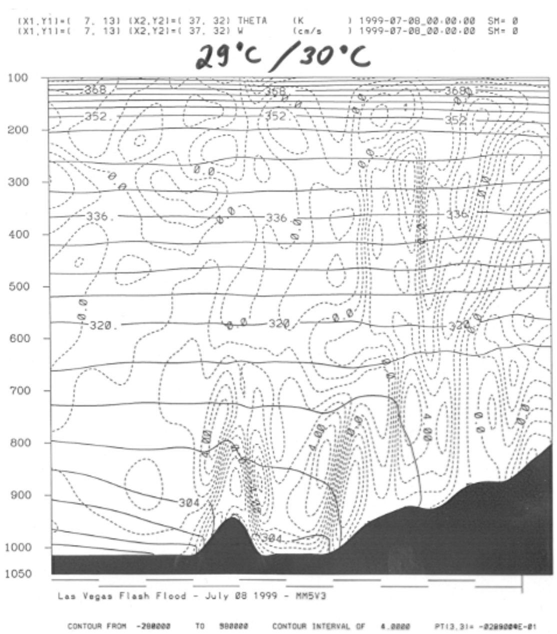

Fig. 9 Simulation 7: 72Z, SW-NE cross-section of potential temperature (K) and updraft vector (m/s)

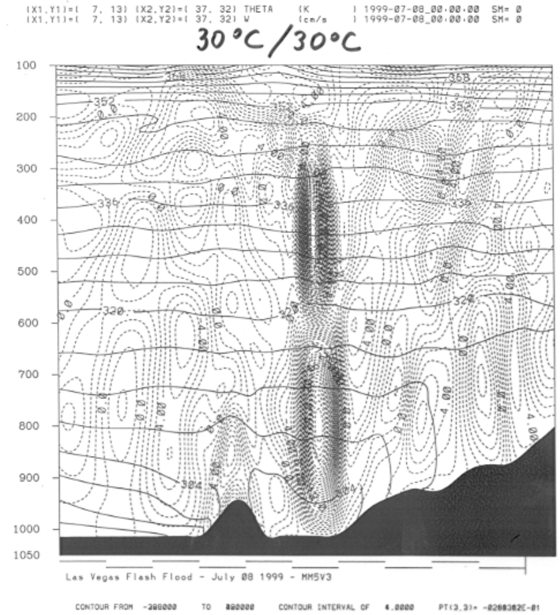

Fig. 10 Simulation 7: 72Z, SW-NE cross-section of potential temperature (K) and updraft vector (m/s)

extensive for simulation 9, when the N.GOC SSTs are only 1 degree higher than in simulation 7.

The precipitable water also increases rapidly over the N. GOC when SSTs increase from 29 to 30°C in the Northern gulf. Low-level mixing ratio fields show hat the GOC is a significant low-level moisture source for monsoonal convection with mixing ratios exceeding 18 g/kg at our cross-section.

At 72Z an interesting development is observed in the potential temperature fields (Fig. 9 and Fig. 10). Much stronger and higher propagating potential temperature gradient is suggesting that the NAM appears to be largely a local divergent monsoon driven by local differential heating. Krishnamurti has reported that NAM does have definable heat sources and sinks, but the scale of those is much smaller than that of the Asian monsoon. He also notes a large diurnal amplitude for the heating and the divergent winds. We plan to investigate further the MM5 potential temperature, wind and cloud water fields.

4. CONCLUSIONS

We performed a series of numerical experiments with the objective of studying if northern GOC SSTs exceeding about 29°C could support favorable monsoonal circulation and BL conditions at adjacent gulf regions and in the U.S. desert southwest.

Our empirical study revealed a rapid increase in rainfall rate over AZNM when N. GOC SSTs exceeded 29°C. Similarly, preliminary MM5 results show a rapid increase in precipitable water over the N. GOC when SSTs increase from 29 to 30°C. This is due to a dilation of the marine boundary layer, apparently resulting from buoyancy driven updrafts prior to and around sunrise, where buoyancy is derived from warmer SSTs and higher mixing ratios of water vapor. MM5 predicted updrafts over Arizona reached the 500 mb level when N. GOC SSTs were 29°C or cooler, but reached 200 mb with a doubling in velocity when SSTs were 30°C. To summarize, both the tropospheric water content and circulation changed dramatically over AZ when the N. GOC SST increased from 29 to 30°C. The model correctly predicted the development of the deep, monsoon PBL.